NASA TECHNICAL NOTE

NASA TN D-4340

EFFECTS OF WALL PRESSURE DISTRIBUTION AND LIQUID TEMPERATURE ON INCIPIENT CAVITATION OF FREON-114 AND WATER IN VENTURI FLOW

by Royce D. Moore, Robert S. Ruggeri, and Thomas F. Gelder

Lewis Research Center
Cleveland, Ohio

NATIONAL AERONAUTICS AND SPACE ADMINISTRATION • WASHINGTON, D. C. • JANUARY 1968

EFFECTS OF WALL PRESSURE DISTRIBUTION AND LIQUID TEMPERATURE ON INCIPIENT CAVITATION OF FREON-114 AND WATER IN VENTURI FLOW

By Royce D. Moore, Robert S. Ruggeri, and Thomas F. Gelder

Lewis Research Center
Cleveland, Ohio

NATIONAL AERONAUTICS AND SPACE ADMINISTRATION

For sale by the Clearinghouse for Federal Scientific and Technical Information
Springfield, Virginia 22151 – CFSTI price $3.00

EFFECTS OF WALL PRESSURE DISTRIBUTION AND LIQUID TEMPERATURE ON INCIPIENT CAVITATION OF FREON-114 AND WATER IN VENTURI FLOW

by Royce D. Moore, Robert S. Ruggeri, and Thomas F. Gelder

Lewis Research Center

SUMMARY

Incipient cavitation of Freon-114 (dichlorotetrafluoroethane) and of water was studied over a range of liquid temperatures in three different transparent venturis mounted in a small hydrodynamic tunnel. Flow velocity in the approach section of the venturis was varied from 18 to 65 feet per second (5.5 to 19.8 m/sec). The venturis were designed to provide systematic changes in wall pressure distribution. Circular arcs of differing radii provided transition from a 1.745-inch- (4.432-cm-) diameter approach section to a 1.375-inch- (3.492-cm-) diameter throat section. For Freon-114, the magnitude of thermodynamic effects of cavitation was significantly reduced for the milder pressure distributions and increased with liquid temperature. No thermodynamic effects of cavitation were observed for water over the temperature range studied. For both water and Freon-114, the incipient cavitation parameter was always less than the noncavitating minimum pressure coefficient, which indicated that the liquids locally experienced effective liquid tensions at the incipient condition. (The incipient cavitation parameter is the ratio of the difference between an upstream reference pressure and the vapor pressure at incipient conditions to the velocity pressure of the upstream flow.) The magnitude of these tensions was strongly dependent on the wall pressure distribution and decreased with the milder pressure distribution.

INTRODUCTION

The development of high-performance propellant pumps has originated from the need to minimize the structural weight of rocket vehicles, specifically, the weight of the propellant tanks. The wall thickness of these tanks is primarily determined by tank pressure, although other factors are involved. Because tank pressure is limited, it is necessary that the propellant be stored at near-saturation conditions. The high-speed pro-

pellant pumps must, therefore, be capable of operation with a low margin of pressure above vapor pressure. To provide this capability, these pumps generally employ an inducer stage that is capable of satisfactory operation at relatively low inlet pressures because of its ability to tolerate considerable amounts of cavitation.

The properties of the liquid and its vapor can have pronounced effects on overall pump cavitation performance. Pumps operated in alcohol, butane, and liquid hydrogen at various temperatures, and in hot water, for example, have lower required margins of inlet pressure above vapor pressure (net positive suction head) than required for the same pumps operated in cold water (refs. 1 to 4). These differences in cavitating performance are generally attributed to the thermodynamic effects of cavitation which reflect the varying degrees of evaporative cooling that accompanies vaporization of the particular liquid being pumped. In situations where evaporative cooling is significant, the cavity pressure and the vapor pressure of the liquid adjacent to the cavity are reduced by an amount corresponding to the reduced local temperature. This reduction in cavity pressure retards the rate of further vapor formation, thereby allowing satisfactory operation of the inducer at lower values of net positive suction head than would otherwise be possible. The magnitude of these thermodynamic effects depends not only on the properties of the liquid, but also on the flow field, that is, local liquid velocities and pressures that influence the degree of the heat and mass transfer involved. In pumps, variations in blade shape, leading edge fairing, and operating conditions such as changes in the blade incidence angle affect the pressure distribution on the blade surface and thus the magnitude of thermodynamic effects.

Studies of thermodynamic effects of cavitation in pumps are, in general, limited to the measurement of changes in overall performance. However, detailed measurements of cavity pressure and temperature as affected by fluid properties and flow velocity have been made in a venturi model (refs. 5 and 6). These studies employed Freon-114 (dichlorotetrafluoroethane) and liquid nitrogen at various temperatures flowing through the same test venturi (fixed pressure distribution). The results showed that cavity temperatures and pressures were substantially less than the temperature and vapor pressure of the bulk liquid by amounts dependent on fluid properties and flow velocity. Furthermore, the magnitude of thermodynamic effect in terms of cavity vapor pressure drop for fixed cavities of near-incipient size was only slightly less than that for more developed cavities. Thus, a study of thermodynamic effects at incipient conditions can provide a qualitative measure of the thermodynamic effects to be expected with developed cavitation.

This investigation evaluates the thermodynamic effects of cavitation at incipient conditions as they are affected by wall pressure distribution and liquid temperature. Freon-114 and water cavitation were studied in three venturis with a 1.375-inch (3.492-cm) throat diameter that differed only in the radii of curvature of the convergence

section. For the tests in which Freon-114 was used, the inlet flow velocity was varied from 18 to 47 feet per second (5.5 to 14.3 m/sec) at controlled temperatures from 0° to 93° F (-17.8° to 33.9° C). The test ranges for water were 18 to 65 feet per second (5.5 to 18.8 m/sec) and 38° to 122° F (3.3° to 50° C). The investigation was conducted at the NASA Lewis Research Center.

APPARATUS

Except for the test sections, the facility used in the present study is the same as that described in detail in references 6 and 7. Briefly, the facility consisted of a small closed-return hydrodynamic tunnel with a capacity of 10 gallons (37.85 liters) and was designed to circulate various liquids by a 700-gallon-per-minute (2650-liter/min) centrifugal pump. The entire tunnel loop was submerged in a bath of ethylene glycol - water mixture that was used to control the tunnel liquid temperature. This bath mixture exchanged heat with a sump-mounted single-tube coil that carried either low-pressure steam or cold nitrogen gas.

The three 12-inch- (30.48-cm-) long venturi test sections (fig. 1) were made of a transparent acrylic plastic, and each had an inlet diameter of 1.745 inches (4.432 cm). The venturis were identical in design except for the contour of the convergence section between the constant diameter approach section and the venturi throat. The convergent wall contours were circular arcs of differing radii, as shown in figure 1, and were chosen to provide a systematic variation in the wall pressure distribution. For the three venturis, the tangency point at the circular arc-throat juncture was located at a fixed distance of 4.383 inches (11.13 cm) from the venturi inlet. The finished contour for the circular arc portion on each venturi is presented in figure 2. The data points represent measured values, as determined on a comparitor, from dental-plaster casts of the venturis. The curves represent the design radii of curvature. Interior surfaces of each venturi test section were highly polished.

Absolute values of the tunnel liquid temperature were measured by means of a calibrated copper-constantan thermocouple mounted on the tunnel centerline approximately 14.5 inches (36.85 cm) upstream from the test section. Test section pressures and the pressure drop across the tunnel contraction nozzle (for determination of test section velocity) were measured with mercury manometers and calibrated precision gages. The accuracy of temperature and gage pressure measurements was $\pm 0.5^{\circ}$ F ($\pm 0.3^{\circ}$ C) and ± 0.15 pounds per square inch (± 0.103 N/cm^2), respectively.

The appearance of vapor cavities was photographed by a still camera in conjunction with a 0.5-microsecond high-intensity flash unit, as well as by a high-speed motion-picture camera. The motion pictures were taken at 6000 frames per second by a 16-millimeter high-speed motion-picture camera coupled to a synchronized light source.

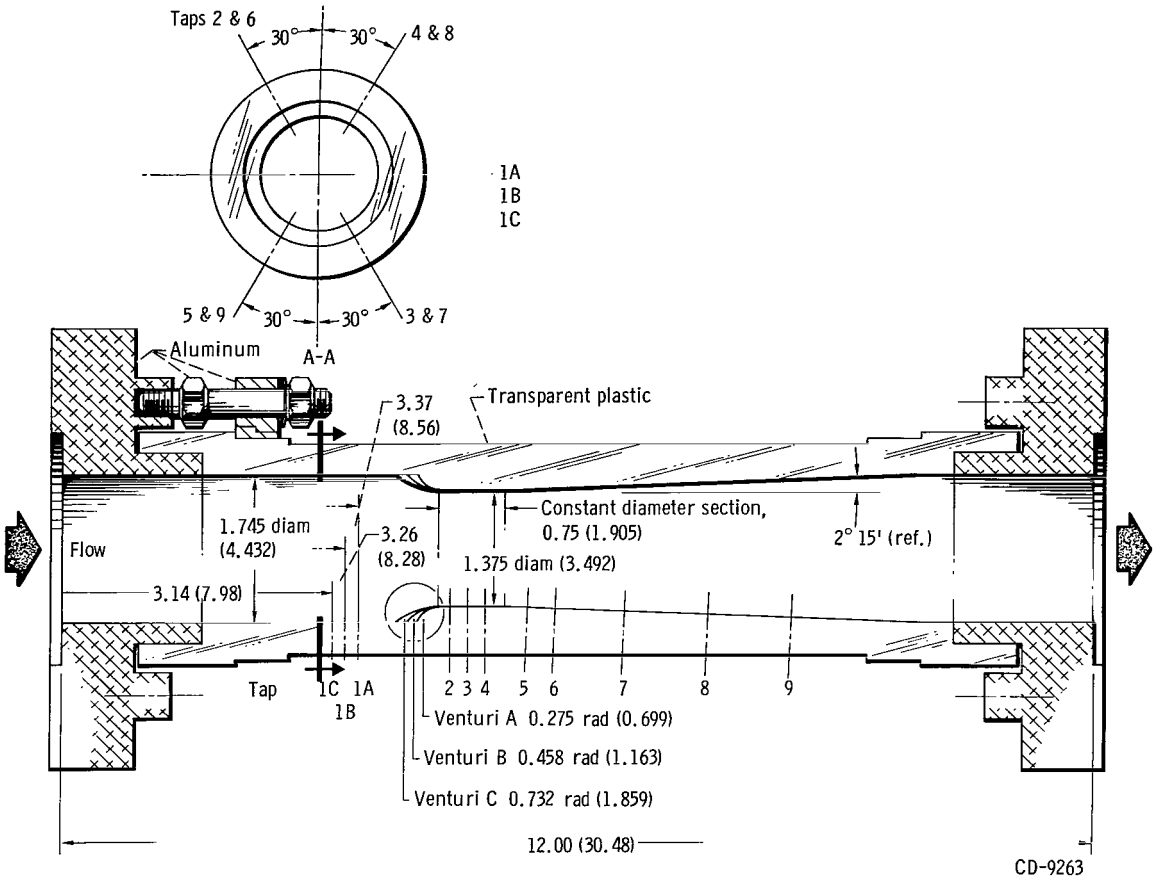

Figure 1. - Venturi test sections showing dimensions and pressure instrumentation (all dimensions are in inches (cm).)

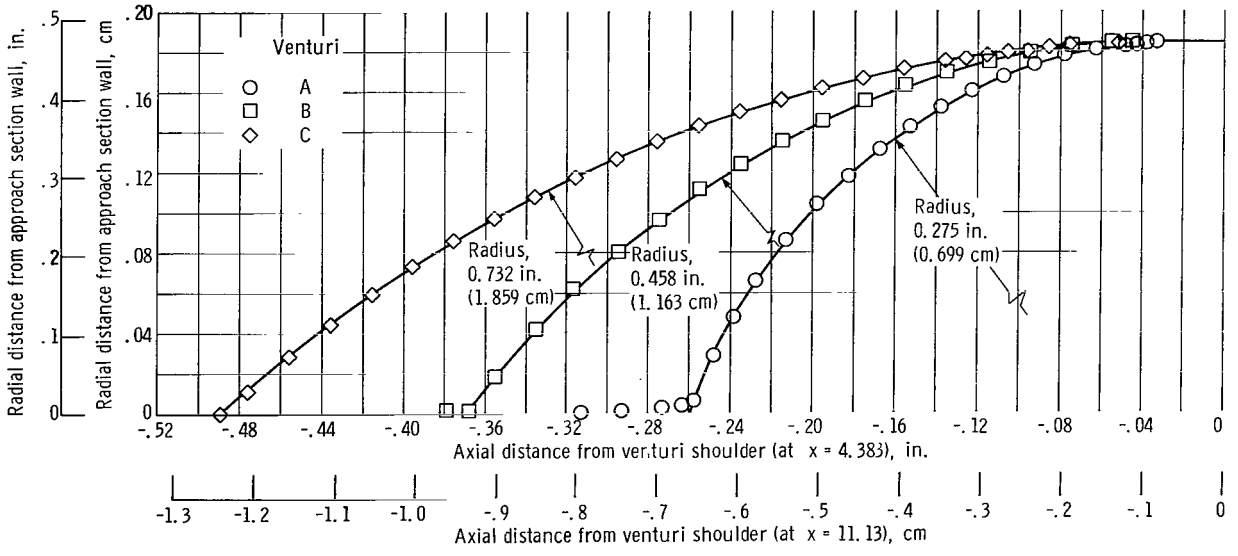

Figure 2. - Measured contours for circular-arc region of venturis.

PROCEDURE

Test Liquids

Freon-114. - A commercial grade of Freon-114 (dichlorotetrafluoroethane) was used as a test liquid. Freon-114 is a clear, colorless liquid that has a normal boiling point of 38.8° F (3.78° C). Some properties of liquid Freon-114 (refs. 8 to 10) are presented for reference in table I. The liquid, which was used directly as received, had a relatively low air content of less than 20 parts per million (ppm) by weight, as specified by the manufacturer. Air-saturated Freon-114 contains about 140 ppm at a temperature of 32° F (0° C) and about 1000 ppm at 0° F (-17.8° C). To minimize contamination by air, the subcooled tunnel and fill lines were evacuated to less than 0.5 millimeter of mercury absolute (66.5 N/m^2 abs) before transferring the Freon-114 to the tunnel.

TABLE I. - PROPERTIES OF FREON-114

(a) U.S. Customary Units

Temperature, °F	Vapor pressure,[a] h_v, ft of Freon-114	Liquid density,[a] lb/cu ft	Vapor density,[b] lb/cu ft	Absolute viscosity,[b] (lb)(sec)/sq ft	Surface tension,[c] lb/ft	Specific heat,[a] Btu/(lb)(°F)	Thermal diffusivity (liquid), ft^2/hr
-20	4.98	100.32	0.127	14.85×10^{-6}	12.73×10^{-4}	0.2105	2.09×10^{-3}
0	8.70	98.50	.210	12.50	11.85	.2171	1.95
20	14.43	96.63	.333	10.77	10.90	.2238	1.84
40	22.92	94.69	.505	9.48	9.93	.2306	1.72
60	35.07	92.69	.738	8.45	9.00	.2372	1.62
80	51.91	90.59	1.048	7.67	8.10	.2435	1.52
100	74.70	88.40	1.438	6.98	7.19	.2498	1.42

(b) SI Units

Temperature, °C	Vapor pressure,[a] h_v, m of Freon-114	Liquid density,[a] g/cu cm	Vapor density,[b] g/cu cm	Absolute viscosity,[b] (N)(sec)/sq m	Surface tension,[c] N/m	Specific heat,[a] cal/(kg)(°C)	Thermal diffusivity (liquid), m^2/hr
-28.9	1.52	1.607	0.00204	7.12×10^{-4}	1.86×10^{-2}	0.2105	1.94×10^{-4}
-17.8	2.65	1.577	.00337	5.99	1.73	.2171	1.81
-6.7	4.40	1.548	.00534	5.16	1.59	.2238	1.71
4.4	7.00	1.516	.0081	4.55	1.45	.2306	1.60
15.6	10.68	1.482	.01182	4.05	1.31	.2372	1.51
26.6	15.82	1.450	.0168	3.68	1.18	.2435	1.41
37.8	22.80	1.416	.0230	3.35	1.05	.2498	1.32

[a]Ref. 8.
[b]Ref. 9.
[c]Ref. 10.

Water. - As in previous venturi cavitation studies (ref. 11), triple-distilled water was used. The water was degassed by boiling in a stainless-steel processing tank prior to its use in the tunnel. For all tests, the air content of water samples taken from the tunnel was less than 3.0 ppm as measured by a conventional Van Slyke apparatus.

Incipient Cavitation Criteria

The initiation of cavitation on the walls of the venturis and the degree of cavitation were controlled by varying the overall liquid pressure level in the tunnel while constant flow velocity and temperature were maintained. From an initial noncavitating state, the liquid pressure was reduced until well-developed cavitation was present. The pressure was then increased slowly until cavitation just disappeared or was intermittent; this condition is defined herein as incipient cavitation. This method of obtaining the incipient condition was used because, in many cases, cavitation obtained at the onset by lowering the pressure was not always the minimum degree of cavitation possible. Characteristics of these cavities at incipient condition are discussed in the section Observations. At the incipient condition, free-stream values of static pressure h_0, velocity V_0, and liquid temperature were measured for determination of the incipient cavitation parameter K_i. (Symbols are defined in the appendix.) All free-stream values refer to an axial location in the venturi approach section about 0.75 inch (1.9 cm) upstream from the start of convergence.

Aerodynamic Studies

To obtain the wall pressure distribution for the critical low-pressure region of the venturis, aerodynamic studies of large accurately scaled models (4.61 scale factor) of the hydrodynamic venturis were made. For the aerodynamic models, 10 pressure taps were located on the critical circular arc portion of the venturi, whereas for the hydrodynamic venturis no pressure taps were installed in the low-pressure region to avoid possible tap cavitation. The aerodynamic models were alined with the airflow in the center of the 6- by 9-foot (1.8- by 2.7-m) test section of the Icing Research Tunnel of the Lewis Research Center.

RESULTS AND DISCUSSION

The noncavitating wall pressure distributions used to evaluate the cavitation data are presented first, followed by the presentation of experimental results. A discussion re-

lating the observed experimental trends to the thermodynamic effects associated with vaporization is then presented. Finally, the visually observed characteristics of Freon-114 and water cavitation at near-incipient conditions are discussed.

Noncavitating Pressure Distribution

The measured axial pressure distribution for the low-pressure region of each venturi is presented in figure 3(a) in terms of the pressure coefficient C_p. All aerodynamic data presented were corrected for compressibility by the method described in reference 12. The minimum values of the pressure coefficient $C_{p,min}$ are -3.35, -2.92, and -2.35 for venturis A, B, and C, respectively. For the three venturis, the location of minimum pressure remained fixed at a value of 2.474 for the ratio of the axial distance from the test section inlet to the free-stream diameter x/D.

The complete axial pressure distribution for venturi B is presented in figure 3(b). For values of x/D greater than about 2.72, the aerodynamic pressure distributions for venturis A and C are the same as that shown for venturi B. Unpublished hydrodynamic data for x/D greater than 2.72 agree with the aerodynamic data of figure 3(b) within 1.0 percent.

Previous studies that used a venturi similar to those studied herein (ref. 11) show that the free-stream Reynolds number Re_D above which $C_{p,min}$ remains constant is about 0.4×10^6. For the hydrodynamic study, the minimum Re_D was approximately 0.2×10^6; however, the results of reference 11 indicate that values of $C_{p,min}$ at this less-than-critical Re_D should not exceed the measured values presented herein by more than 2.0 percent. Because this change is small and the greater portion of the water data and all the Freon-114 data were obtained at values of Re_D exceeding 0.4×10^6, the value of $C_{p,min}$ for each venturi is considered constant throughout.

Incipient Cavitation

The conventional incipient cavitation parameter is used herein to denote the liquid and flow conditions at which cavitation disappears as stream pressure is slowly increased at a constant flow velocity,

$$K_i \equiv \frac{h_0 - h_v}{\frac{V_0^2}{2g}}$$

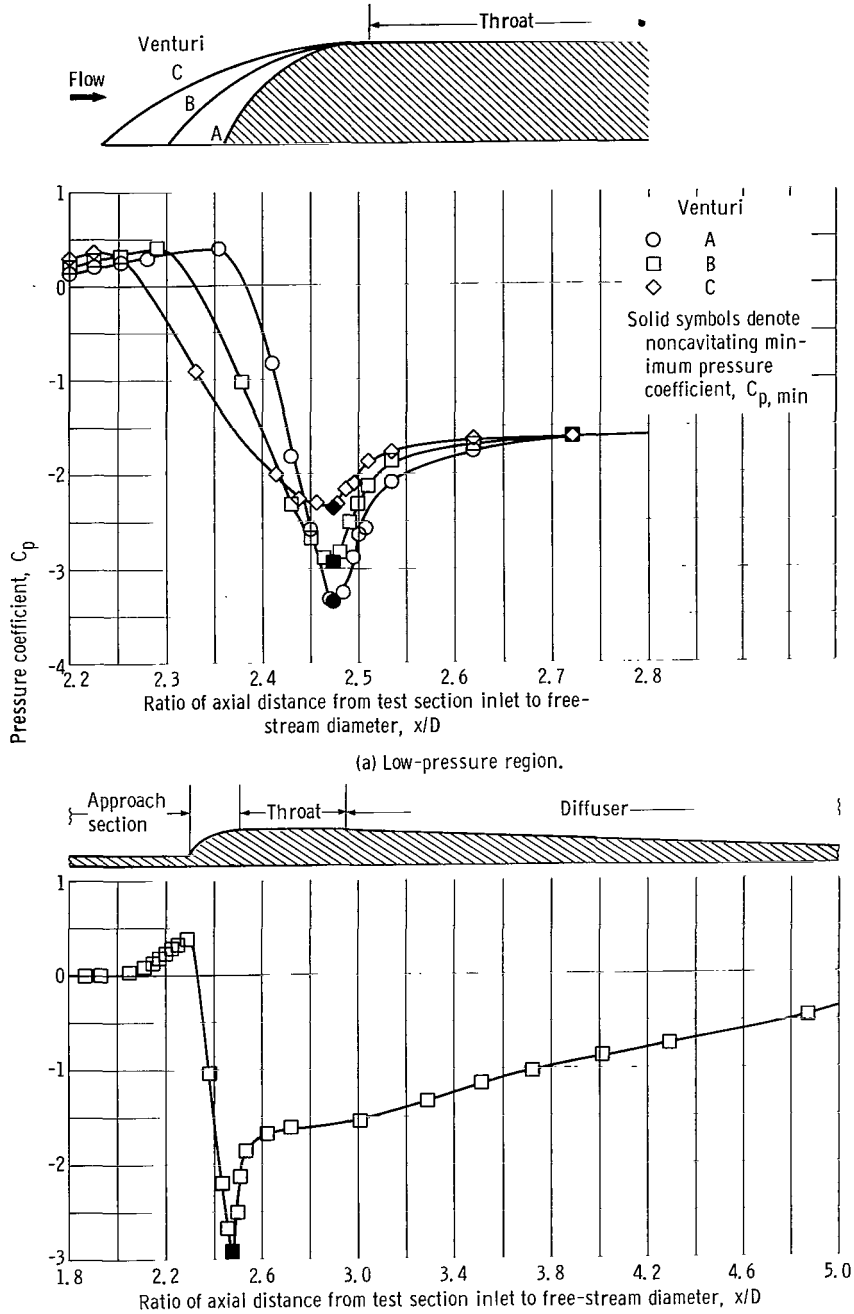

(a) Low-pressure region.

(b) Complete wall pressure distribution for venturi B.

Figure 3. - Noncavitating venturi wall pressure distribution. Aerodynamic data for 4.61-scale venturi models.

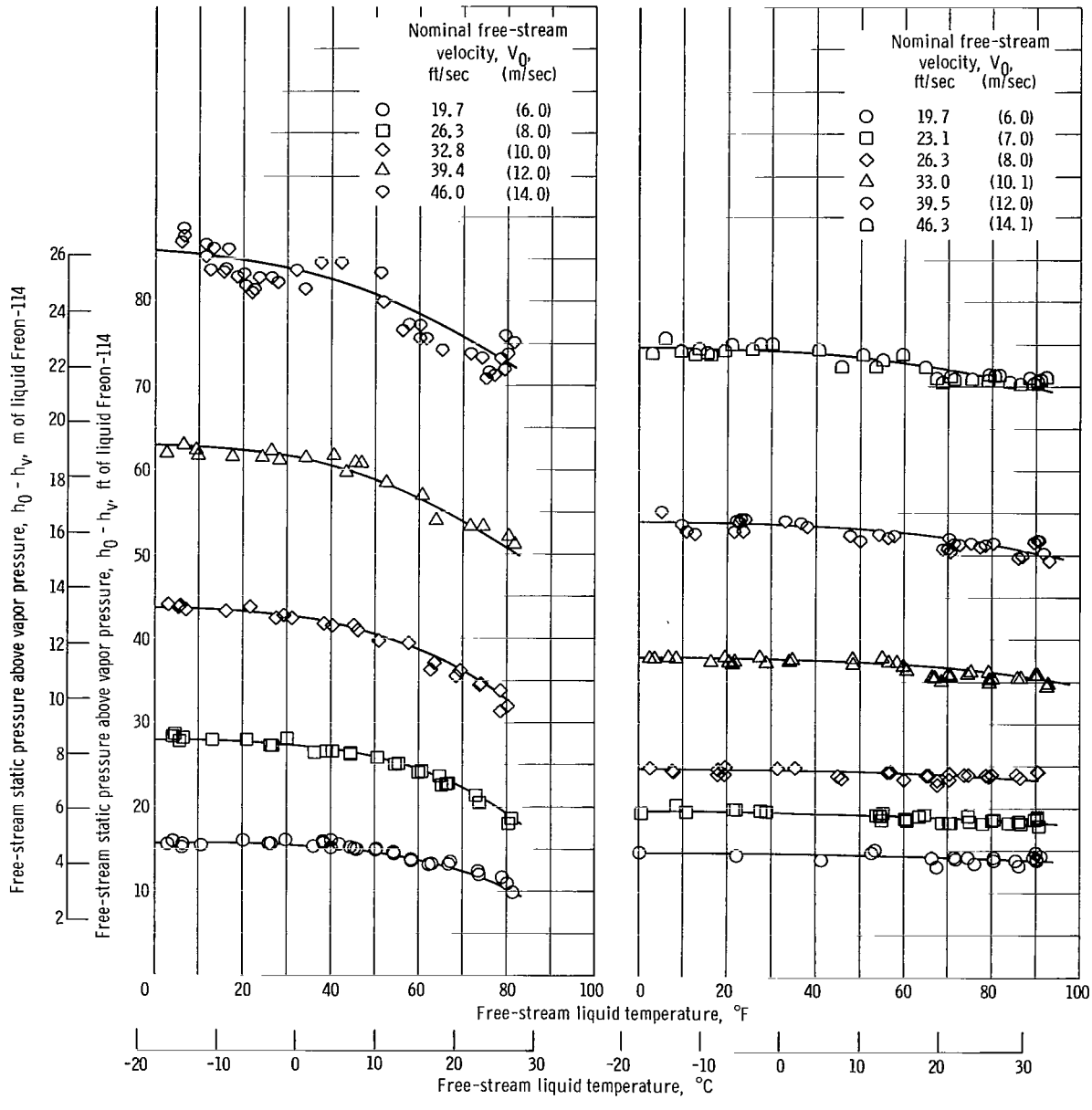

(a) Venturi A. (b) Venturi C.

Figure 4. - Free-stream static pressure above vapor pressure at incipient cavitation for Freon-114 as function of free-stream liquid temperature for several free-stream velocities.

The basic data used to evaluate K_i for Freon-114 in venturis A and C are presented in figure 4, where the numerator of K_i is shown plotted as a function of liquid temperature for several free-stream velocities. For the free-stream velocities studied, the effect of temperature is greater for venturi A than for venturi C.

No data were obtained for Freon-114 in venturi B because exposure to Freon-114 caused the inside surfaces of this model to craze; thus, only water data are presented for this venturi.

Values from the faired curves of figure 4 were used to calculate values of the incipient cavitation parameter K_i, shown in figure 5 as a function of stream velocity, for arbitrarily chosen liquid temperatures of 0^o, 40^o, and 80^o F (-17.8^o, 4.4^o, and 26.7^o C).

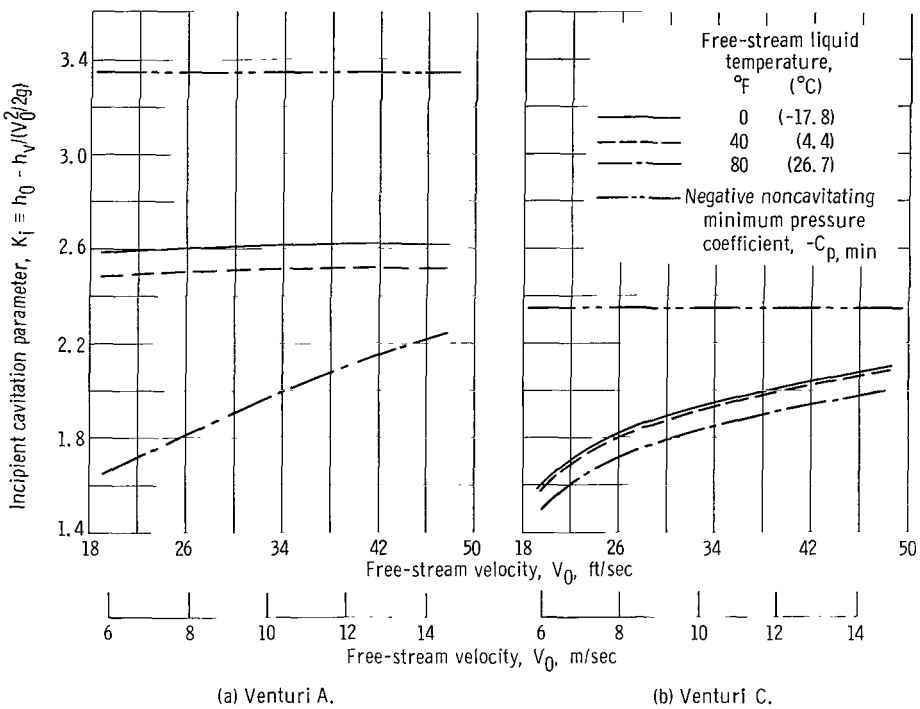

Figure 5. - Incipient cavitation parameter for Freon-114 (from data fairing of fig. 4) as function of free-stream velocity and liquid temperature.

The negative of the noncavitating minimum pressure coefficient is also shown for use later in the discussion. The data for both venturis A and C show similar trends of increasing values of K_i with increasing free-stream velocity.

For venturis A and C, the values of the incipient cavitation parameter decreased with increasing liquid temperature with a comparatively greater decrease observed at the higher temperature. Venturi A, which had the more severe wall pressure distribution, showed a greater decrease in K_i for a given increase in temperature than did venturi C.

The incipient cavitation parameter for water in venturis A, B, and C is presented in figure 6 as a function of free-stream velocity for nominal water temperatures of 40^o, 75^o,

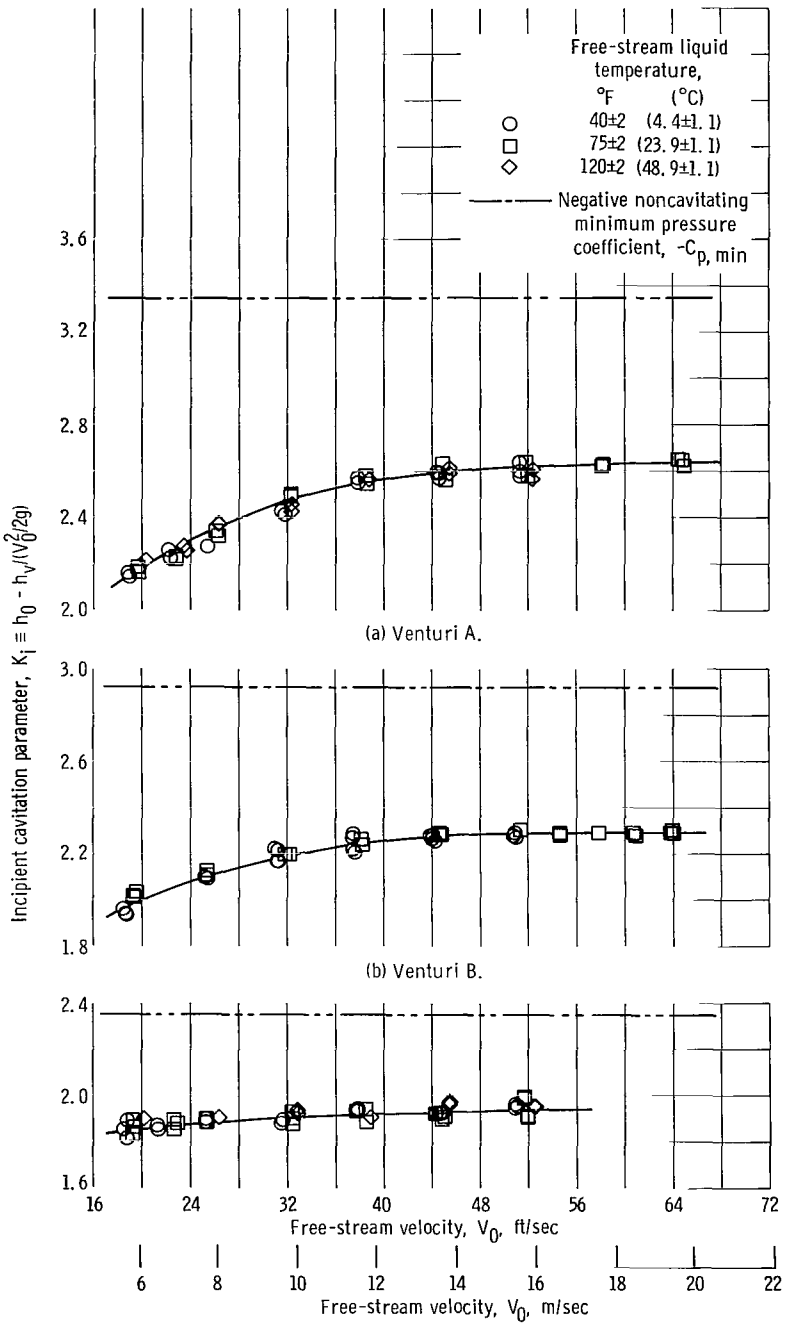

Figure 6. - Incipient cavitation parameter for water as function of free-stream velocity and liquid temperature.

and 120° F (4.4°, 23.9°, and 48.9° C). For each venturi, the K_i values increased with increasing velocity and approached a constant value at the higher velocities. No measureable effect of water temperature on K_i was observed for the range of temperature studied. These results indicate that the variation in the cavitation parameter with flow velocity decreases with the less severe wall pressure distributions.

If incipient cavitation occurs when the minimum pressure h_{min} equals the vapor pressure corresponding to stream temperature h_v, the cavitation parameter K_i must, by definition, correspond to the negative of the $C_{p,min}$ value. The experimental cavitation results presented in figures 5 and 6 show that K_i values were always appreciably less than $-C_{p,min}$, thus, the minimum pressure was always less than vapor pressure at incipient conditions. For this condition, $h_{min} < h_v$, effective liquid tension can be considered to exist within the liquid (ref. 6). The sum, $K_i + C_{p,min}$ (a negative quantity) is a measure of the maximum effective liquid tension in terms of the velocity head $V_0^2/2g$, and the value of tension is then

$$h_{min} - h_v = \frac{V_0^2}{2g}(K_i + C_{p,min})$$

This relation assumes that the noncavitating value of $C_{p,min}$ is valid at incipient conditions. Effective liquid tensions based on the faired K_i curves for water (fig. 6) and Freon-114 (fig. 5) are presented in figures 7 and 8, respectively.

The curves of the effective liquid tension obtained with water for the three venturis (fig. 7) are similar; tensions increase rapidly with increasing flow velocity and are independent of liquid temperature for the range studied. The magnitude of effective water tension progressively decreases as the pressure distribution becomes less severe.

Water tension values tend to increase with the more severe pressure distributions and with increasing stream velocity. This tendency is consistent with the concept that the growth of a moving bubble at incipient conditions is dependent on both the length of time that the fluid is exposed to local pressures less than free-stream vapor pressure and the magnitude of these pressure decrements (ref. 13). The total time that the liquid along the wall is exposed to pressures less than free-stream vapor pressure is herein termed exposure time. During the exposure time, the liquid experiences a range of tensions that vary between 0 (where $h_x = h_v$) and the maximum values presented in figures 7 and 8. Exposure time was calculated with the use of surface distance and an averaged velocity within that region where local pressures were less than stream vapor pressure. Exposure time is shown on auxiliary scales in figures 7 and 8. At a given velocity, the exposure times for water are less for venturi A than for venturi C because of the shorter surface distance across the low-pressure region (see fig. 3(a), p. 8).

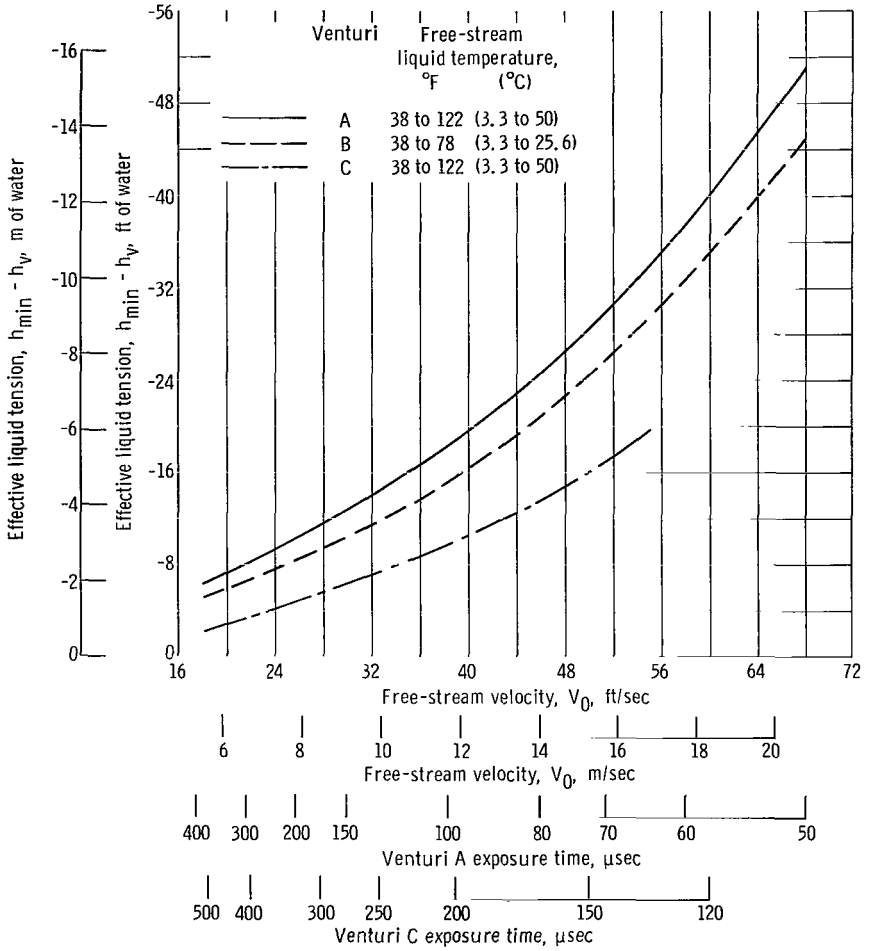

Figure 7. - Effective liquid tension for water corresponding to incipient cavitation.

The curves of effective liquid tension for Freon-114 in venturis A and C (fig. 8) show similar trends with respect to both flow velocity and liquid temperature. The effective liquid tensions noted for venturi A, which has the more severe pressure distribution, are as much as three times the corresponding values obtained for venturi C; and temperature effects are also significantly greater for venturi A.

For Freon-114, the increasing values of tension with increasing temperature are attributed to the greater reduction in cavity pressure at the higher temperatures caused by the thermodynamic effects of cavitation (as discussed in the next section). Because the reduction in cavity pressure and, thus, the retardation in bubble growth rate are greater at higher temperature, longer exposure times are required for Freon-114 at the higher temperatures (fig. 8).

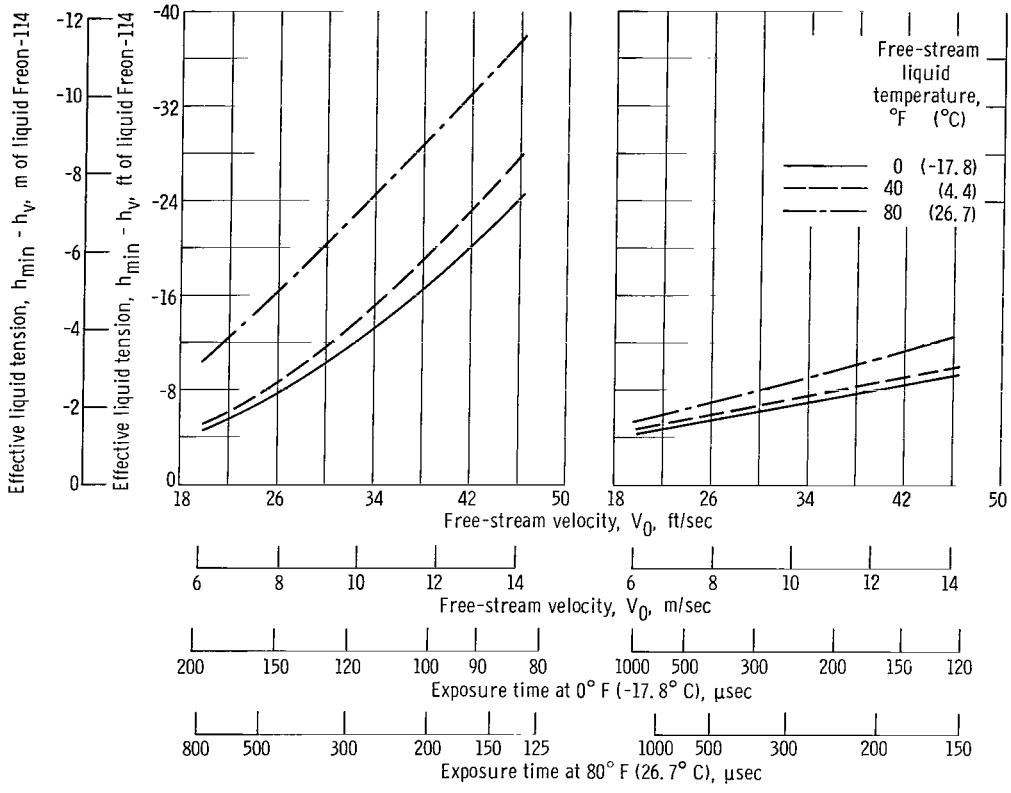

(a) Venturi A. (b) Venturi C.

Figure 8. - Effective liquid tension for Freon-114 corresponding to incipient cavitation.

Thermodynamic Effects of Cavitation

A microscopic bubble begins to grow when the local pressure falls below the local vapor pressure, and it continues to grow as long as the local pressures are less than vapor pressure. As the vapor bubble grows, the heat required for vaporization must be drawn from the surrounding liquid. In a flowing system, the length of time that the vapor bubble experiences pressures less than vapor pressure is usually short. Therefore, the region of liquid supplying the heat for vaporization is confined to a relatively thin layer of liquid adjacent to the cavity. The resultant cooling of this liquid film causes a decrease in vapor pressure within the vapor bubble corresponding to the reduced film temperature, provided that thermodynamic equilibrium conditions are established and no permanent gases are present. This decrease in cavity pressure reduces the bubble growth rate. Analyses of bubble growth in flowing systems show that the magnitude of the cavity pressure depression within a growing bubble depends on fluid properties. Bubble growth is also a function of wall pressure distribution, flow velocity, and the heat- and mass-transfer mechanisms involved (refs. 13 and 14). For the purpose of this discussion,

other factors that influence bubble growth, such as viscosity and surface tension, have been neglected.

The fluid properties that control the degree of vapor pressure depression within a cavity include the heat of vaporization, the specific heat and thermal diffusivity of the liquid, and the liquid and vapor densities.

For a vapor bubble of a given size at incipient conditions, the mass of vapor generated, and thus the amount of heat required for vaporization of a given liquid, can differ by several orders of magnitude over a temperature range because of changes in vapor density. As a result of the increased vapor density that accompanies the increased vapor pressure at higher temperature, the mass of vapor for a given volume is increased. For a given body geometry and flow velocity, the mass of the liquid contained in the thin layer of liquid supplying the heat for vaporization remains essentially constant because of the small change with temperature in the thermal diffusivity of a given liquid. More heat is required to generate the increased mass of vapor, and this heat is drawn from a mass of liquid that remains essentially constant. Thus, a greater temperature drop, with a correspondingly greater cavity pressure depression, is realized at higher temperatures. The growth-retarding effect of lowered cavity pressure results in a reduction of the stream pressure for which the vapor bubbles will grow to the visible size corresponding to incipient conditions. Thus, because of the thermodynamic effects of cavitation, values of the incipient cavitation parameter K_i decrease with increasing temperature, as noted in reference 5 and herein (fig. 5, p. 10) for Freon-114.

In the present investigation, Freon-114 showed marked thermodynamic effects whereas, in water, the effect was negligible. These differences are attributed primarily to differences in the vapor density of the two fluids. For the temperature range covered in the water tests, the density of water vapor was about 1/50 to 1/2500 of that for Freon-114 vapor; thus the heat required for the vaporization of water was too small to cause a measureable thermodynamic effect. Differences in other fluid properties were small by comparison.

Changes in body contour alone (changes in the pressure coefficient variations) influence the thermodynamic effects of cavitation in a manner similar to that of varying free-stream velocity over a given body geometry. For either case, the magnitude of the thermodynamic effects is strongly dependent on the thickness of the liquid layer supplying the heat of vaporization. Liquid layer thickness is a function of the thermal diffusivity of the liquid and the time available for bubble growth. For the milder pressure distributions associated with bodies having larger radii of curvature or for relatively low flow velocities, the liquid is exposed to pressures less than free-stream vapor pressure for relatively longer periods of time. As a result, the temperature gradient due to evaporative cooling penetrates further into the liquid surrounding the cavity. Since the same total heat for vaporization is in this case drawn from a greater mass of liquid, the reductions

in cavity temperature and corresponding vapor pressure are less.

Previous venturi studies of Freon-114 cavitation show that the thermodynamic effects of cavitation may be evaluated qualitatively from the measured variations in K_i with temperature. In the study of reference 5, free-stream pressure was reduced until well-developed cavities were formed. Measurements of the local pressure in the cavitated region of Freon-114 and liquid nitrogen were made over a range of temperature and free-stream velocity; in this way, a direct evaluation of the depression in cavity pressure caused by the thermodynamic effects of cavitation was obtained. In addition, if the cavity pressure at incipient conditions was used instead of free-stream vapor pressure, the incipient cavitation parameter had a constant value (independent of temperature) for each particular velocity, that is,

$$K_{ic} = \frac{h_0 - h_c}{\frac{V_0^2}{2g}} = \frac{h_0 - (h_v - \Delta h_v)}{\frac{V_0^2}{2g}} = K_i + \frac{\Delta h_v}{\frac{V_0^2}{2g}} = \text{Const}$$

Therefore

$$K_i = \text{Const} - \frac{\Delta h_v}{\frac{V_0^2}{2g}}$$

The incipient cavitation parameter K_i is thus directly related to the cavity pressure depression Δh_v.

If the preceding relation is assumed to hold for the venturis of this investigation, the thermodynamic effects of cavitation can be evaluated qualitatively on the basis of the relative difference in K_i values with temperature. For Freon-114, the relative difference in K_i values with temperature is greater for venturi A (fig. 5(a), p. 10) than that for venturi C (fig. 5(b)) at all flow velocities. These differences indicate that the cavity pressure depressions and thus the thermodynamic effects of cavitation in Freon-114 are greater for models that have the more severe wall pressure distributions because of the shorter periods of time available for bubble growth.

The results of reference 5 show that for Freon-114 the reduction in cavity pressure due to the thermodynamic effects of cavitation was less than 1.0 foot (0.3 m) at 5° F (-15° C) for a venturi that had a more severe pressure distribution than venturi A. Thus, the tension values obtained for Freon-114 at 0° F (-17.8° C) in both venturis A and C (fig. 8) essentially represent the tension values for Freon-114 with no thermodynamic

effects of cavitation present. This occurrence of tension in the absence of thermodynamic effects for Freon-114 at 0° F (-17.8° C), and other liquids as well, is attributed to the finite times required for the nucleation and growth of a bubble to visible size. The thermodynamic effects of cavitation can be a substantial part of effective tension; for example, in venturi A (fig. 8(a)), the thermodynamic effects of cavitation for Freon-114 at 80° F (26.7° C) and 20 feet per second (6.1 m/sec) account for about one-half the effective liquid tension obtained. In contrast, for venturi C under similar conditions, that portion of effective tension contributed by thermodynamic effects is significantly less. The results of figure 8 indicate that, for mild pressure distributions (with corresponding longer exposure times), the thermodynamic effects of cavitation can be insignificant, even for a liquid that might ordinarily be expected to yield large thermodynamic effects when considered on the basis of the fluid properties alone.

Observations

The appearance of water and Freon-114 cavitation at incipient conditions varied considerably with the venturi shape, flow velocity, and liquid temperature; however, the appearance of cavitation can be categorized into the four basic types illustrated in figure 9. In the following discussion, free-stream Reynolds number Re_D is used in describing observations of cavitation; however, the use of Re_D is for convenience only and is not intended to demonstrate its usefulness as a correlating parameter.

For free-stream Reynolds numbers Re_D of less than approximately 1.0×10^6, the last appearance of cavitation for Freon-114 in venturi A and for water in venturis A and B consisted of a complete ring of individual vapor cavities about 1/16 to 1/8 inch long (0.16 to 0.32 cm long) around the periphery of the venturi, as shown in figure 9(a). For Re_D values greater than 1.0×10^6, both water and Freon-114 cavitation changed from the ring type (fig. 9(a)) to that illustrated in figure 9(b), where the vapor cavities were in the form of intermittent flashes that appeared randomly about the periphery of the venturi. For Freon-114 and water data obtained for venturis A and B, the cavities were fixed with the cavity leading edge always located at or near the point of minimum pressure.

For venturi C, all water cavities and most Freon-114 cavities at the incipient level appeared as one or two intermittent flashes at or near the point of minimum pressure, as shown in figure 9(c). The one exception was noted with Freon-114 at temperatures greater than 80° F (26.7° C) and free-stream velocities of less than 25 feet per second (7.6 m/sec). For these conditions, the last visible cavitation was observed to occur usually in the venturi throat about 1/2 to 3/4 inch (1.27 to 1.90 cm) downstream from the point of minimum pressure (see fig. 9(d)). Motion pictures taken at about 6000 frames per second showed that these last visible cavities actually originated as small vapor bub-

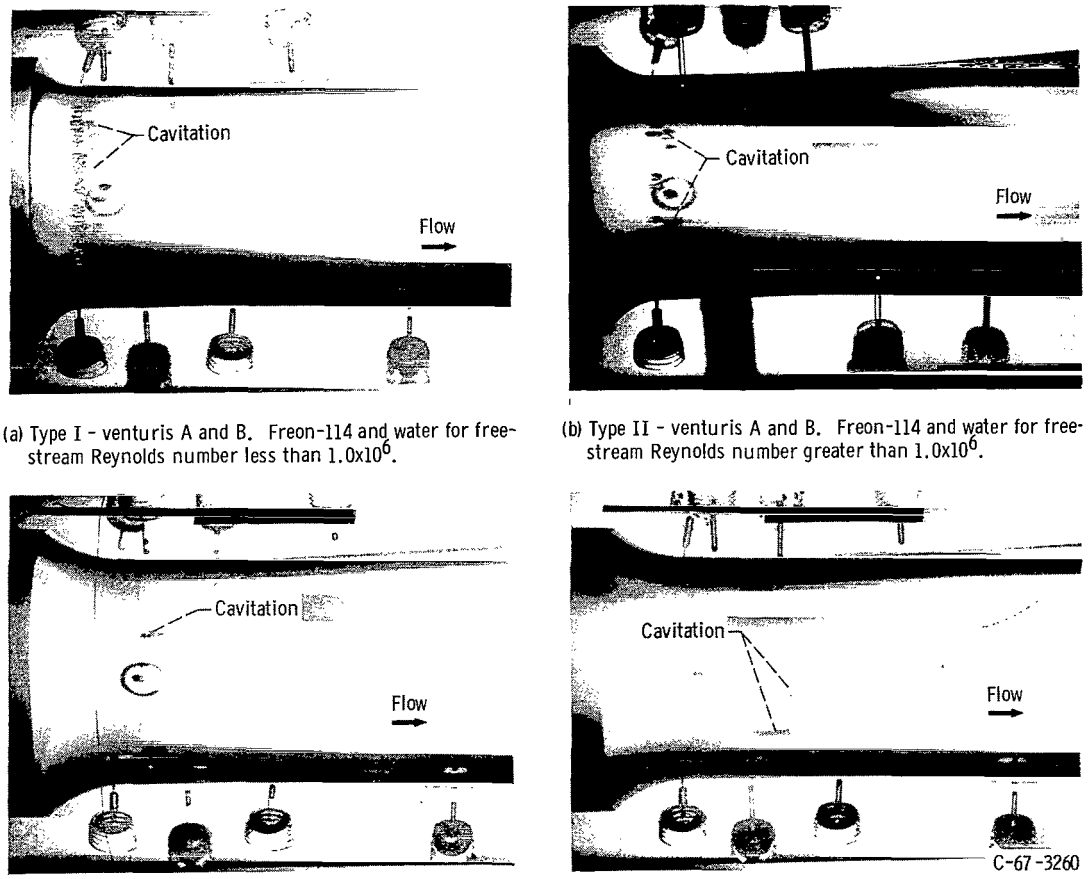

(a) Type I - venturis A and B. Freon-114 and water for free-stream Reynolds number less than 1.0×10^6.

(b) Type II - venturis A and B. Freon-114 and water for free-stream Reynolds number greater than 1.0×10^6.

(c) Type III - venturi C. Freon-114 for temperature less than 80° F (26.7° C) and free-stream velocity greater than 25 feet per second (7.6 m/sec). Water for all conditions studied.

(d) Type IV - venturi C. Freon-114 for temperature greater than 80° F (26.7° C) and free-stream velocity less than 25 feet per second (7.6 m/sec).

Figure 9. - Appearance of various types of Freon-114 and water cavitation at near-incipient conditions.

bles formed at or near the minimum pressure location; these bubbles then traveled about 1/2 inch (1.27 cm) downstream before growing to a size visible to the unaided eye. The occurrence of traveling cavities probably resulted from a combination of sizable thermodynamic effects at 80° F (26.7° C) and the rather mild absolute pressure distribution that accompanies the lower velocities; both of these conditions retard the bubble growth rate. The low values of K_i at the high-temperature low-speed conditions indicate that the wall pressures in the venturi throat at incipient conditions were considerably less than free-stream vapor pressure, which accounts for the presence of vapor bubbles downstream of the minimum pressure region.

CONCLUDING REMARKS

The present study indicates that the thermodynamic effects of cavitation are greater

for the more severe wall pressure distributions. Although these results were obtained with the use of venturis, a similar trend might be expected to occur with other flow devices such as pumps and inducers.

The leading edge fairing of pump or inducer blades has little effect on the overall pressure rise of the pump. However, the fairing does influence the pressure distribution in the critical low-pressure region on the blade suction surface. Thus, from previous discussion, a sharp leading edge fairing, such as commonly used for inducer blades, would provide a more severe pressure distribution locally than would a smooth radius fairing and consequently might be expected to yield the greater thermodynamic effects of cavitation under the same flow conditions.

Pumps and inducers are generally required to operate over a range of flows. As the flow rate is varied at a fixed rotative speed, the incidence angle changes. As a result, the blade pressure distribution is altered, and, therefore, the thermodynamic effects of cavitation might be expected to vary accordingly.

Although the predicted trends in thermodynamic effects with changes in blade leading edge fairing and pump flow conditions are based on venturi cavitation results, it appears reasonable to assume that these trends are likely to occur in pumps. However, systematic pump cavitation studies are needed to substantiate these conclusions further.

SUMMARY OF RESULTS

Incipient cavitation of Freon-114 (dichlorotetrafluoroethane) and of water was studied over a range of flow velocity and liquid temperature in three different tunnel-mounted venturis. The venturis were of identical design except for the contour of the convergent section, which consisted of circular arcs with radii of 0.275 inch (0.699 cm), 0.458 inch (1.163 cm), and 0.732 inch (1.859 cm). The venturi approach section and throat diameters were 1.745 inches (4.432 cm) and 1.375 inches (3.492 cm), respectively. This study yielded the following principal results:

1. For Freon-114, the magnitude of the thermodynamic effects of cavitation, as measured by the variation in the incipient cavitation parameter K_i with temperature, was significantly greater for the venturi having the most severe wall pressure distribution. The K_i values for water were unaffected by temperature, which indicated that the thermodynamic effects were negligible over the temperature range studied, 38° to 122° F (3.3° to 50° C).

2. The incipient cavitation parameter was always less than the noncavitating minimum pressure coefficient, which indicated that the liquids locally experienced effective liquid tensions at the incipient conditions. The magnitude of these tensions was strongly dependent on the wall pressure distribution. For the same temperature and free-stream

velocity, tension values for the venturi with the 0.275-inch (0.699-cm) contour radius were as much as three times larger than those for the venturi with the 0.732-inch (1.859-cm) radius.

3. For Freon-114 in each venturi, values of the incipient cavitation parameter decreased with increasing temperature over the temperature range studied, 0° to 93° F (-17.8° to 33.9° C). The decrease in the cavitation parameter was greater at the higher temperatures.

Lewis Research Center,
National Aeronautics and Space Administration,
Cleveland, Ohio, September 12, 1967,
128-31-06-28-22.

APPENDIX - SYMBOLS

C_p	noncavitating pressure coefficient, $(h_x - h_0)/(V_0^2/2g)$
$C_{p,min}$	noncavitating minimum pressure coefficient, $(h_{min} - h_0)/(V_0^2/2g)$
D	free-stream diameter, 1.745 in.; 4.432 cm
g	acceleration due to gravity, 32.2 ft/sec^2; 9.8 m/sec^2
h_c	pressure in cavitated region, ft of liquid abs; m of liquid abs
h_{min}	noncavitating minimum static pressure (see fig. 3, p. 8), ft of liquid abs; m of liquid abs
h_v	vapor pressure corresponding to free-stream liquid temperature, ft of liquid abs; m of liquid abs
Δh_v	reduction in cavity pressure due to thermodynamic effects of cavitation, ft of liquid; m of liquid
h_x	wall static pressure at x/D, ft of liquid abs; m of liquid abs
h_0	free-stream static pressure (venturi approach section), ft of liquid abs; m of liquid abs
K_i	incipient cavitation parameter based on free-stream vapor pressure, $(h_0 - h_v)/(V_0^2/2g)$
K_{ic}	incipient cavitation parameter based on cavity pressure, $(h_0 - h_c)/(V_0^2/2g)$
Re_D	free-stream Reynolds number, $V_0 D/\nu$
V_0	free-stream velocity, ft/sec; m/sec
x	axial distance from test section inlet, in.; cm
ν	kinematic viscosity based on free-stream liquid temperature, ft^2/sec; m^2/sec

REFERENCES

1. Spraker, W. A.: The Effects of Fluid Properties on Cavitation in Centrifugal Pumps. Paper No. 64-WA/FE-14, ASME, Nov. 1964.
2. Stepanoff, A. J.: Cavitation in Centrifugal Pumps with Liquids Other than Water. J. Eng. Power, vol. 83, no. 1, Jan. 1961, pp. 79-90.
3. Salemann, Victor: Cavitation and NPSH Requirements of Various Liquids. J. Basic Eng., vol. 81, no. 2, June 1959, pp. 167-173.
4. Ball, Calvin L.; Meng, Phillip R.; and Reid, Lonnie: Cavitation Performance of 84° Helical Pump Inducer Operated in 37° and 42° R Liquid Hydrogen. NASA TM X-1360, 1967.
5. Gelder, Thomas F.; Ruggeri, Robert S.; and Moore, Royce D.: Cavitation Similarity Considerations Based on Measured Pressure and Temperature Depressions in Cavitated Regions of Freon-114. NASA TN D-3509, 1966.
6. Ruggeri, Robert S.; and Gelder, Thomas F.: Cavitation and Effective Liquid Tension of Nitrogen in a Tunnel Venturi. NASA TN D-2088, 1964.
7. Ruggeri, Robert S.; and Gelder, Thomas F.: Effects of Air Content and Water Purity on Liquid Tension at Incipient Cavitation in Venturi Flow. NASA TN D-1459, 1963.
8. Van Wie, Nelson H.; and Ebel, Robert A.: Some Thermodynamic Properties of Freon-114. Vol. 1. -40° F to the Critical Temperature. Rep. No. K-1430, AEC, Sept. 2, 1959.
9. Anon.: "Freon." Products Div. Bull. T114B, E. I. duPont de Nemours Co., Inc.
10. Anon.: "Freon." Products Div. Bull. D-27, E. I. duPont de Nemours and Co., Inc.
11. Ruggeri, Robert S.; Moore, Royce D.; and Gelder, Thomas F.: Incipient Cavitation of Ethylene Glycol in a Tunnel Venturi. NASA TN D-2722, 1965.
12. Gelder, Thomas F.; Moore, Royce D.; and Ruggeri, Robert S.: Incipient Cavitation of Freon-114 in a Tunnel Venturi. NASA TN D-2662, 1965.
13. Parkin, Blaine R.: Scale Effects in Cavitating Flow. Rep. No. 21-8, Hydrodynamics Lab., California Inst. Tech., July 31, 1952.
14. Plesset, M. S.; and Zwick, S. A.: A Nonsteady Heat Diffusion Problem with Sperical Symmetry. J. Appl. Phys., vol. 23, no. 1, Jan. 1952, pp. 95-98.

"The aeronautical and space activities of the United States shall be conducted so as to contribute . . . to the expansion of human knowledge of phenomena in the atmosphere and space. The Administration shall provide for the widest practicable and appropriate dissemination of information concerning its activities and the results thereof."

—NATIONAL AERONAUTICS AND SPACE ACT OF 1958

NASA SCIENTIFIC AND TECHNICAL PUBLICATIONS

TECHNICAL REPORTS: Scientific and technical information considered important, complete, and a lasting contribution to existing knowledge.

TECHNICAL NOTES: Information less broad in scope but nevertheless of importance as a contribution to existing knowledge.

TECHNICAL MEMORANDUMS: Information receiving limited distribution because of preliminary data, security classification, or other reasons.

CONTRACTOR REPORTS: Scientific and technical information generated under a NASA contract or grant and considered an important contribution to existing knowledge.

TECHNICAL TRANSLATIONS: Information published in a foreign language considered to merit NASA distribution in English.

SPECIAL PUBLICATIONS: Information derived from or of value to NASA activities. Publications include conference proceedings, monographs, data compilations, handbooks, sourcebooks, and special bibliographies.

TECHNOLOGY UTILIZATION PUBLICATIONS: Information on technology used by NASA that may be of particular interest in commercial and other non-aerospace applications. Publications include Tech Briefs, Technology Utilization Reports and Notes, and Technology Surveys.

Details on the availability of these publications may be obtained from:

SCIENTIFIC AND TECHNICAL INFORMATION DIVISION

NATIONAL AERONAUTICS AND SPACE ADMINISTRATION

Washington, D.C. 20546